Computational and Structural Biotechnology Journal 20 (2022) 380–384

COMPUTATIONAL AND STRUCTURAL BIOTECHNOLOGY JOURNAL

journal homepage: www.elsevier.com/locate/csbj

Communications

Homologous cardiac calcium pump regulators phospholamban and sarcolipin adopt distinct oligomeric states in the membrane

Andy Y. Liu [a,b], Rodrigo Aguayo-Ortiz [c], Guadalupe Guerrero-Serna [a], Nulang Wang [a], Muriel G. Blin [d], Daniel R. Goldstein [d,e,f], L. Michel Espinoza-Fonseca [a,d,*]

[a] Center for Arrhythmia Research, Division of Cardiovascular Medicine, University of Michigan, Ann Arbor, MI 48109, USA
[b] McKetta Department of Chemical Engineering, The University of Texas, Austin, TX 78712, USA
[c] Departamento de Farmacia, Universidad Nacional Autónoma de México, Mexico City 04510, Mexico
[d] Department of Internal Medicine, University of Michigan, Ann Arbor, MI 48109, USA
[e] Department of Microbiology and Immunology, University of Michigan, Ann Arbor, MI 48109, USA
[f] Institute of Gerontology, University of Michigan, Ann Arbor, MI 48109, USA

ARTICLE INFO

Article history:
Received 26 October 2021
Received in revised form 18 December 2021
Accepted 21 December 2021
Available online 28 December 2021

Keywords:
Calcium pump
Phospholamban
Sarcolipin
Oligomerization
Cardiac calcium regulation
Membrane proteins

ABSTRACT

Phospholamban (PLN) and Sarcolipin (SLN) are homologous membrane proteins that belong to the family of proteins that regulate the activity of the cardiac calcium pump (sarcoplasmic reticulum Ca^{2+}-ATPase, SERCA). PLN and SLN share highly conserved leucine zipper motifs that control self-association; consequently, it has been proposed that both PLN and SLN assemble into stable pentamers in the membrane. In this study, we used molecular dynamics (MD) simulations and Western blot analysis to investigate the precise molecular architecture of the PLN and SLN oligomers. Analysis showed that the PLN pentamer is the predominant oligomer present in mouse ventricles and ventricle-like human iPSC-derived cardiomyocytes, in agreement with the MD simulations showing stable leucine zipper interactions across all protomer-protomer interfaces and MD replicates. Interestingly, we found that the PLN pentamer populates an asymmetric structure of the transmembrane region, which is likely an intrinsic feature of the oligomer in a lipid bilayer. The SLN pentamer is not favorably formed across MD replicates and species of origin; instead, SLN from human and mouse atria primarily populate coexisting dimeric and trimeric states. In contrast to previous studies, our findings indicate that the SLN pentamer is not the predominant oligomeric state populated in the membrane. We conclude that despite their structural homology, PLN and SLN adopt distinct oligomeric states in the membrane. We propose that the distinct oligomeric states populated by PLN and SLN may contribute to tissue-specific SERCA regulation via differences in protomer–oligomer exchange, oligomer–SERCA dynamics, and noise filtering during β-adrenergic stimulation in the heart.

1. Introduction

Phospholamban (PLN) and Sarcolipin (SLN) are homologous membrane proteins that belong to the family of proteins that regulate the activity of the calcium pump (sarcoplasmic reticulum Ca^{2+}-ATPase, SERCA)[1]. In the heart, PLN is expressed abundantly in ventricles [2], whereas SLN is found in the atria [3,4]. Spectroscopy studies have shown that PLN and SLN form homo-oligomers with high-order stoichiometry [5]. Previous studies have suggested that oligomerization serves as storage from which the active protomers binding to SERCA are released [6]. More recently, we used complementary electron cryo-electron microscopy, biochemical analyses, and atomistic simulations to show that PLN and SLN homo-oligomers directly interact with SERCA with different functional outcomes: PLN homo-oligomers increase the maximal activity of the pump [7], whereas SLN homo-oligomers decrease the maximal activity of SERCA [8]. These studies underline the importance of PLN and SLN oligomerization for the regulation of SERCA-mediated calcium transport in the heart.

Abbreviations: SERCA, sarcoplasmic reticulum Ca^{2+}-ATPase;; PLN, phospholamban; SLN, sarcolipin; MD, molecular dynamics; iPSC, induced pluripotent stem cells; POPC, 1-palmitoyl-2-oleoyl-*sn*-glycero-3-phosphocholine.

* Corresponding author.
E-mail address: lmef@umich.edu (L. Michel Espinoza-Fonseca).

https://doi.org/10.1016/j.csbj.2021.12.031

PLN and SLN share similar motifs that control self-association and oligomer stoichiometry [9,10], and previous studies have shown that both PLN and SLN assemble into stable and symmetrical pentamers in the membrane [11–14]. In apparent contradiction with this view, spectroscopy studies have shown that PLN, but not SLN, self-associate into distinct pentamers [15], and that SLN dimers and higher-order oligomeric may coexist in a membrane environment [9]. In this study, we used microsecond-long atomistic molecular dynamics (MD) simulations and western blot analysis of atrial and ventricular tissue to investigate the precise molecular architecture of the PLN and SLN oligomers.

We point out that the published NMR structure of human SLN is only available for the protomer (PDB: 1jdm [16]); given the homology between SLN and PLN, we build a structure of the SLN pentamer using the NMR structure of the PLN pentamer as a template (PDB: 2kyv [11], Fig. 1A). In the final model, each SLN protomer crosses the lipid bilayer with a tilt angle of ∼11° about the membrane normal (Fig. 1B). Like the PLN pentamer, the modeled structure of the SLN pentamer is characterized by a cyclic point symmetry with the axis running perpendicular to the membrane plane. We also point out that the SLN pentamer generated in this study is nearly identical to that reported in previous computational studies [12–14]; accordingly, we used this structure as an initial model to perform five independent 1-μs MD simulations of the SLN pentamer in a lipid bilayer composed of POPC lipids. In addition, we performed four independent 1-μs MD simulations of the PLN pentamer starting from the most representative structures extracted from the NMR ensemble.

We plotted the distributions over the tilt angle for each protomer calculated for each snapshot in the MD trajectories to establish a blueprint for the preferred configuration of the protomers in the PLN and SLN pentamers. We found that the configuration of the PLN and SLN pentamers deviates substantially from that measured in the initial structure of the oligomers. In the PLN pentamer, the protomers show a broad spread of tilt angles in the microsecond-long trajectories, ranging from 0° to 40° (Fig. 1C). Similarly, the SLN protomers in most trajectories populate tilt angles between 0° and 50° (Fig. 1D). Reconfiguration of individual PLN and SLN protomers is accompanied by either a fractional or full loss in the cyclic point symmetry that is characteristic of the modeled and NMR structures of the PLN and SLN pentamers, respectively (Fig. 2). In the PLN pentamer, the transition toward a mostly asymmetric structure of the transmembrane region occurs in all four trajectories; for instance, protomers M2 and M3 retain an average angle of 11°, whereas protomers M1, M4, and M5 undergo a shift toward a larger transmembrane tilt angle (tilt angle of 22–25°, Fig. 1C and Fig. 2A). The SLN pentamer modeled here also adopts a mostly asymmetric structure of the transmembrane domain: SLN protomers in replicates 2, 3, and 5 have dissimilar average tilt angles that translate into a unique configuration of the individual transmembrane helices of the protomers (Fig. 1D and Fig. 2B). We observed a moderate reconfiguration of all protomers in replicate 1; however, the average tilt angles for each protomer in this replicate are similar, thus suggesting that SLN may form symmetric pentamers (Fig. 1D and Fig. 2B). Interestingly, asymmetry of the SLN oligomer was also observed in a single 0.5 μs MD trajectory previously reported by us [8]. Together, these findings suggest that the PLN and SLN pentamers are intrinsically asymmetric, in contrast with previous reports proposing that the pentameric form primarily populates a cyclic symmetry [11]. A possible explanation for this difference is that Xplor-NIH, the software that was used for NMR structure determination of the PLN pentamer [11], uses distance symmetry restraint protocols that favor a cyclic symmetry packing [17]. It is therefore possible that the asymmetry observed here is an intrinsic characteristic of the SLN and PLN pentamers in a lipid bilayer environment because our simulations were performed in the absence of these restraints.

We analyzed the stability of the pentamers by quantifying the stability of a conserved leucine zipper that is essential for the oligomerization of PLN and SLN [9,10]. To this aim, we plotted the distributions of the distances Ile40–Leu37 and Ile40–Leu44 (for PLN) and Ile17–Ile14 and Ile17–Leu21 (for SLN) across all protomer–protomer interfaces in the MD trajectories. A leucine zipper is considered stable only if both residue-residue distances satisfy a value of ∼7 Å; this cutoff value is based on the residue-residue distance calculated from the initial model of the NMR structure of the PLN pentamer [11]. Analysis of the trajectories shows that the leucine zipper in the PLN pentamer is stable across all protomer–pro-

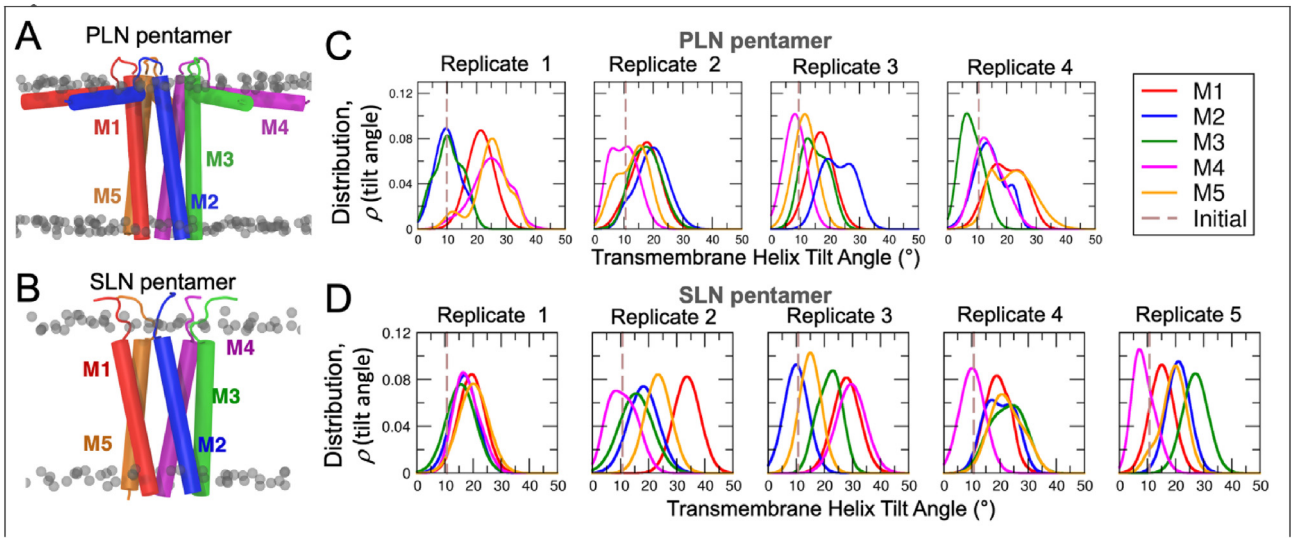

Fig. 1. Molecular architecture of the PLN and SLN pentamers in a lipid bilayer. (A) A representative structure from the NMR ensemble of the PLN pentamer (PDB: 2kyv [11]). (B) The three-dimensional structure of the SLN pentamer we used as a starting point for the MD simulations. Distributions of the tilt angle of the transmembrane domain of each (C) PLN and (D) SLN protomer were calculated from the MD trajectories using the pentamer as a starting structure. The dashed line indicates the average tilt angle calculated for all protomers using the initial structures of the PLN and SLN pentamers. In all cases, individual protomers M1 (red), M2 (blue), M3 (green), M4 (magenta), and M5 (orange) are shown in a cartoon representation. (For interpretation of the references to colour in this figure legend, the reader is referred to the web version of this article.)

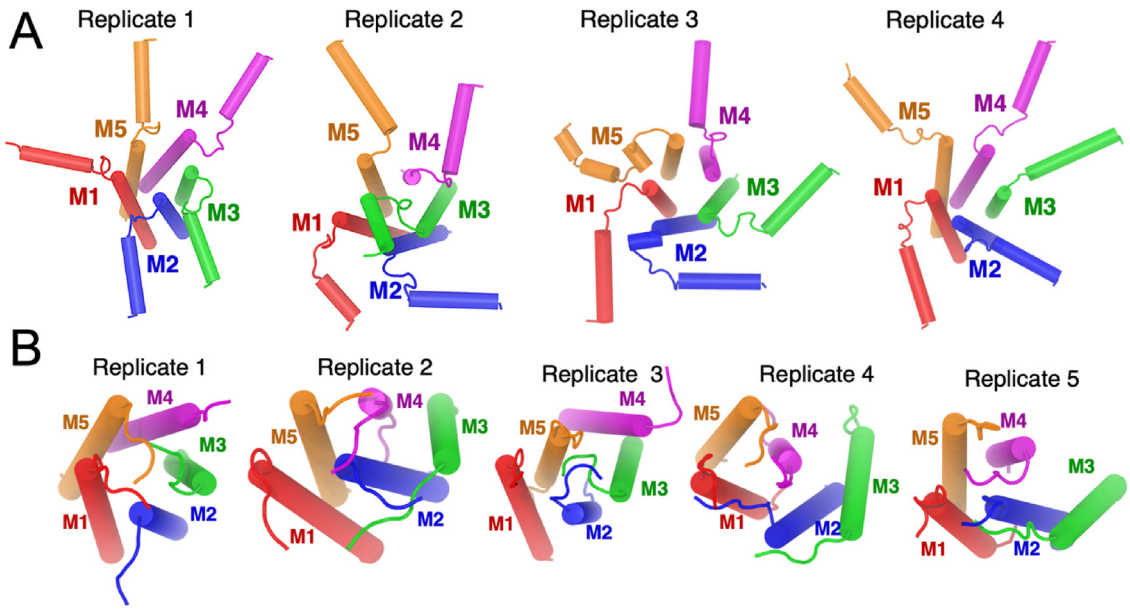

Fig. 2. Structures of the PLN and SLN pentamers. (A) Structures of the PLN pentamer at the end of the 1-μs MD trajectory. (B) Configuration of the SLN pentamer at the end of each MD replicate. In all cases, the structures are oriented so that the z-axis is parallel to the membrane plane normal and viewed from the cytosolic side. Individual protomers M1 (red), M2 (blue), M3 (green), M4 (magenta), and M5 (orange) are shown in a cartoon representation. (For interpretation of the references to colour in this figure legend, the reader is referred to the web version of this article.)

tomer interfaces and independent replicates (Fig. 3 and Fig. S1, Supplemental material) and that the stability is independent of the asymmetric structure of the pentamer detected in the simulations. In contrast to the PLN pentamer, we found that the leucine zipper is not stably formed across all protomer–protomer interfaces in most MD replicates of the SLN pentamers. Indeed, the leucine zipper of the SLN pentamer is either transiently formed (e.g., between protomers M2–M3 of replicate 2, Fig. 3), or is completely disrupted (e.g., between protomers M3–M4 of replicate 4, Fig. 3). The full set of protomer–protomer interresidue distances calculated from the simulations of the SLN pentamer are reported in Fig. S2 of Supplemental material.

Previous studies have shown that the N-terminus of SLN plays functional roles in SERCA regulation[18,19] and interdomain communication [20]. In this study, we found that the N-termini of SLN may interact with each other in the oligomers (Fig. 2B). However,

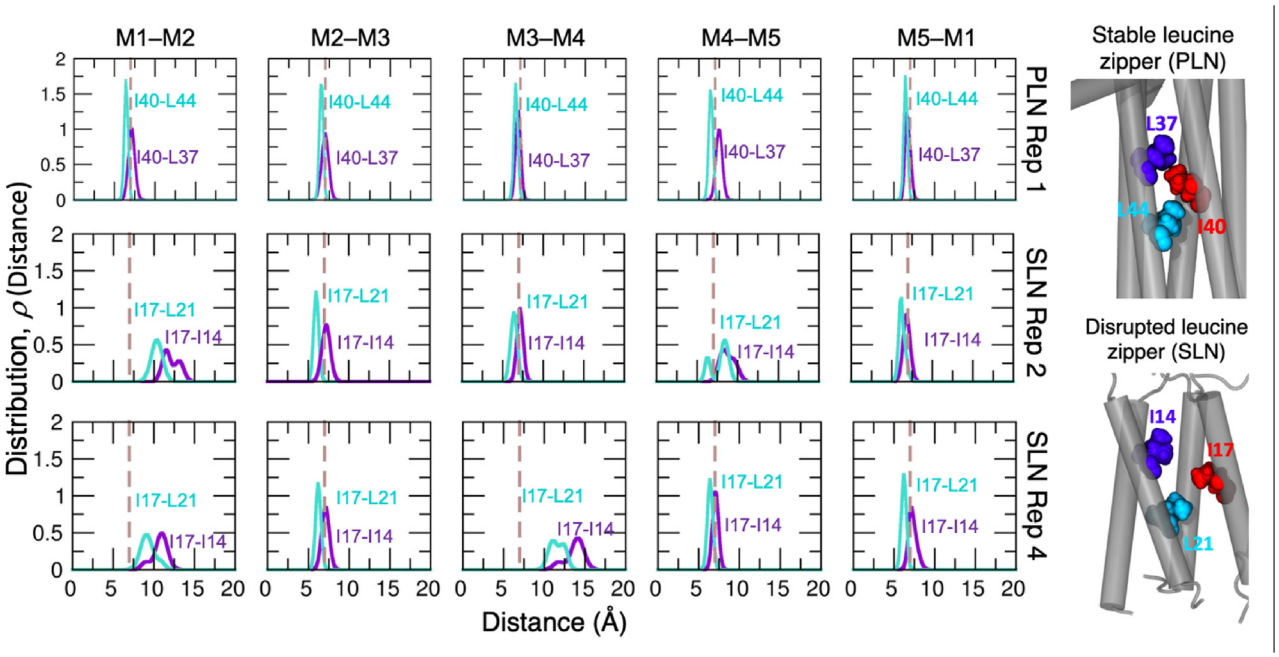

Fig. 3. Stability of the leucine zipper, measured by key interresidue distance distributions across all protomer–protomer interfaces. We show selected interresidue distances calculated from replicate 1 of PLN and replicates 2 and 4 of SLN. The dashed brown line indicates the average distance calculated from the initial model of the SLN pentamer as well as the NMR structure of the PLN pentamer. Each interface is labeled using the nomenclature used in Figs. 1 and 2. The representations on the left panel show the PLN and SLN pentamers (cartoon representation) and the location of the leucine zipper residues (van der Waals spheres). These structures also illustrate stable and disrupted leucine zippers.

these interactions do not appear functional because the close contact between the N-termini of adjacent protomer does not result in stable protein-protein contacts in the transmembrane domain. For instance, helices M4 and M5 in replicate 2 of the SLN pentamer are in proximity (Fig. 2B), but these protomers do not form stable leucine zippers in the simulation (Fig. 3).

We performed Western blot analysis of mouse heart and human iPSC-derived cardiomyocytes as a complementary approach to verify the high-resolution structural information obtained from the MD simulations. Western blot analysis showed that the PLN pentamer is the predominant oligomer present in both mouse ventricles and human iPSC-derived cardiomyocytes (Fig. 4A). These findings agree with the stability of leucine zipper interactions across all protomer–protomer interfaces and replicates of the PLN pentamer (Fig. 4B and Fig. S1). Conversely, we did not conclusively find a band corresponding to the SLN pentamer in either mouse atria or human iPSC-derived atrial cardiomyocytes. Instead, we found the presence of the SLN dimer and trimer in mouse atria, and the dimer and pentamer in human iPSC-derived atrial cardiomyocytes (Fig. 4C). MD simulations agree with experiments and show that the SLN pentamer breaks down primarily into dimers and trimers (Fig. 4D). We performed additional MD simulations to verify the stability of individual dimeric and trimeric forms of SLN oligomers and demonstrate that these oligomers are stabilized by specific protomer–protomer leucine zipper interactions (Figs. S3-S4, Supplemental material). While it can be argued that the SLN pentamer may exist in other organisms, we performed additional MD simulations to demonstrate that the pentamer formed by mouse SLN is not structurally stable in the microsecond time scale (**Figs. S5-S6,** Supplemental material). These findings, which are reproducible across replicates, species of origin, and primary antibodies (Figs. S7-S8), are in contrast with previous studies suggesting that pentamers are the primary oligomeric form of SLN in the membrane [12–14]. There is excellent agreement between simulations and experiments demonstrating that the pentamer is the main oligomeric form of PLN, whereas SLN primarily populates coexisting dimeric and trimeric states in the membrane. We note that we detected a band that corresponds to the SLN pentamer in both mouse atria and human iPSC-derived atrial cardiomyocytes. This finding is consistent with the formation of the SLN pentamer in a single MD trajectory. These findings suggest that SLN pentamers may form in cardiac cells, albeit less frequently than other oligomeric states populated in the membrane. It is reasonable to argue that the lipid composition of the sarcoplasmic reticulum in atrial and ventricular tissue contributes to the differences in oligomerization between PLN and SLN. However, we rule out this possibility as the phospholipid composition is similar in microsomal fractions of atria and ventricles [21,22].

In summary, we demonstrated that despite their structural homology, PLN and SLN adopt distinct oligomeric states in the membrane. Our study provides new functional and structural hypotheses that can be tested both with simulations and experimentally. For example, previous studies have shown that high expression of PLN and SLN have significantly cytotoxic effects, with SLN having a more potent cytotoxic effect in *vitro*. There is evidence showing that the presence of several oligomeric states correlates with higher cytotoxicity [23], so our findings may provide a mechanistic explanation for these differences since SLN populates a broader range of homo-oligomers than PLN. The differences in oligomerization and symmetry found here may also explain the divergence in SERCA regulation either via protomer–oligomer exchange [5], oligomer–SERCA dynamics [7,8], and to ensure con-

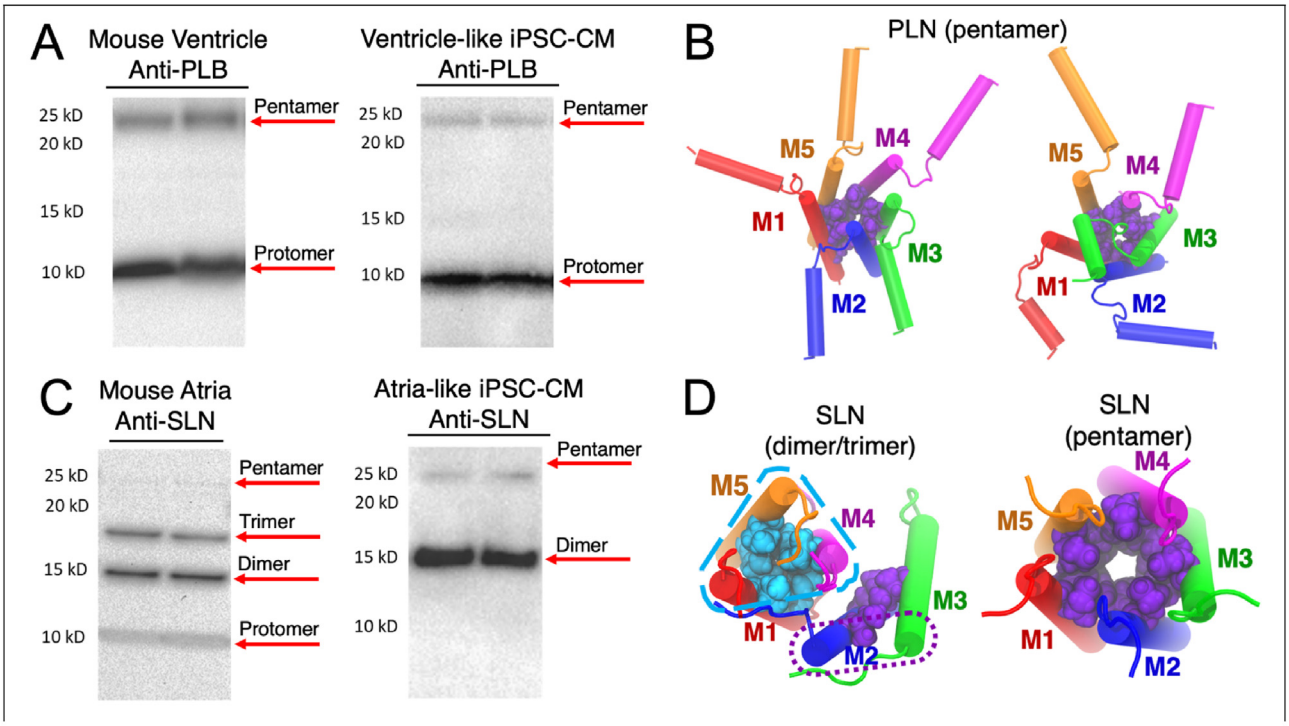

Fig. 4. Oligomerization of PLN and SLN in mouse hearts and human iPSC-derived cardiomyocytes (iPSC-CM) revealed by Western blot analysis. (A) Western blot analysis of mouse ventricles and ventricle-like human iPSC-derived cardiomyocytes showed the presence of PLN pentamers in both species. (B) Representative structures of the PLN pentamer (cartoon representation) show the formation of stable leucine zippers (purple spheres). (C) We detected the presence of SLN dimers, trimers, and pentamers in mouse atria, whereas dimers and pentamers were found in atria-like human iPSC-derived cardiomyocytes. (D) MD simulations of the SLN oligomers agree with experiments and revealed the formation of structurally stable dimeric, trimeric and pentameric states. Individual protomers are shown in a cartoon representation, and leucine zippers are shown as spheres. (For interpretation of the references to colour in this figure legend, the reader is referred to the web version of this article.)

sistent protomer phosphorylation during β-adrenergic stimulation [24]. Finally, we propose that the degeneracy of structural states that have been associated with membrane protein asymmetry [25] may be of importance for allosteric regulation and functional adaptation of SERCA by PLN in the heart [26,27]. These functional mechanisms, which can be tested using computer simulations in concert with mutagenesis, spectroscopy, and cell-based assays, will provide new insights into the functional contribution of PLN and SLN oligomerization to cardiac function in health and disease.

Declaration of Competing Interest

The authors declare that they have no known competing financial interests or personal relationships that could have appeared to influence the work reported in this paper.

Acknowledgments

We thank the Frankel Cardiovascular Regeneration Core Laboratory at the University of Michigan for providing us with human iPSC-derived atrial cardiomyocytes. A.Y.L. was supported by a University of Michigan Frankel Cardiovascular Center Summer Undergraduate Research Fellowship. This study was funded by the National Institutes of Health grants R01GM120142 (to L.M.E.-F), and R01AG028082, R35HL155169 and R01AI138347 (to D.R. G.). This research was supported in part through computational resources and services provided by Advanced Research Computing at the University of Michigan, Ann Arbor, Michigan.

Appendix A. Supplementary data

Supplementary data to this article can be found online at https://doi.org/10.1016/j.csbj.2021.12.031.

References

[1] Bhupathy P, Babu GJ, Periasamy M. Sarcolipin and phospholamban as regulators of cardiac sarcoplasmic reticulum Ca2+ ATPase. J Mol Cell Cardiol 2007;42(5):903–11.
[2] Koss KL, Kranias EG. Phospholamban: a prominent regulator of myocardial contractility. Circ Res 1996;79(6):1059–63.
[3] Minamisawa S, Wang Y, Chen Ju, Ishikawa Y, Chien KR, Matsuoka R. Atrial chamber-specific expression of sarcolipin is regulated during development and hypertrophic remodeling. J Biol Chem 2003;278(11):9570–5.
[4] Babu GJ, Bhupathy P, Timofeyev V, Petrashevskaya NN, Reiser PJ, Chiamvimonvat N, et al. Ablation of sarcolipin enhances sarcoplasmic reticulum calcium transport and atrial contractility. Proc Natl Acad Sci U S A 2007;104(45):17867–72.
[5] Singh DR, Dalton MP, Cho EE, Pribadi MP, Zak TJ, Seflova J, et al. Newly Discovered Micropeptide Regulators of SERCA Form Oligomers but Bind to the Pump as Monomers. J Mol Biol 2019;431:4429–43.
[6] Becucci L, Cembran A, Karim CB, Thomas DD, Guidelli R, Gao J, et al. On the function of pentameric phospholamban: ion channel or storage form? Biophys J 2009;96(10):L60–2.
[7] Glaves JP, Primeau JO, Espinoza-Fonseca LM, Lemieux MJ, Young HS. The Phospholamban Pentamer Alters Function of the Sarcoplasmic Reticulum Calcium Pump SERCA. Biophys J 2019;116(4):633–47.
[8] Glaves JP, Primeau JO, Gorski PA, Espinoza-Fonseca LM, Lemieux MJ, Young HS. Interaction of a Sarcolipin Pentamer and Monomer with the Sarcoplasmic Reticulum Calcium Pump. SERCA. Biophys J 2020;118(2):518–31.
[9] Autry JM, Rubin JE, Pietrini SD, Winters DL, Robia SL, Thomas DD. Oligomeric interactions of sarcolipin and the Ca-ATPase. J Biol Chem 2011;286(36):31697–706.
[10] Simmerman HKB, Kobayashi YM, Autry JM, Jones LR. A leucine zipper stabilizes the pentameric membrane domain of phospholamban and forms a coiled-coil pore structure. J Biol Chem 1996;271(10):5941–6.
[11] Verardi R, Shi L, Traaseth NJ, Walsh N, Veglia G. Structural topology of phospholamban pentamer in lipid bilayers by a hybrid solution and solid-state NMR method. Proc Natl Acad Sci U S A 2011;108(22):9101–6.
[12] Cao Y, Wu X, Lee I, Wang X. Molecular dynamics of water and monovalent-ions transportation mechanisms of pentameric sarcolipin. Proteins 2016;84(1):73–81.
[13] Cao Y, Wu X, Wang X, Sun H, Lee I. Transmembrane dynamics of the Thr-5 phosphorylated sarcolipin pentameric channel. Arch Biochem Biophys 2016;604:143–51.
[14] Cao Y, Yang R, Sun J, Zhang W, Lee I, Wang W, et al. Effects of amino acid modifications on the permeability of the pentameric sarcolipin channel. Proteins 2021;89(4):427–35.
[15] Hellstern S, Pegoraro S, Karim CB, Lustig A, Thomas DD, Moroder L, et al. Sarcolipin, the shorter homologue of phospholamban, forms oligomeric structures in detergent micelles and in liposomes. J Biol Chem 2001;276(33):30845–52.
[16] Mascioni A, Karim C, Barany G, Thomas DD, Veglia G. Structure and orientation of sarcolipin in lipid environments. Biochemistry 2002;41(2):475–82.
[17] Schwieters CD, Kuszewski JJ, Tjandra N, Marius Clore G. The Xplor-NIH NMR molecular structure determination package. J Magn Reson 2003;160(1):65–73.
[18] Autry JM, Thomas DD, Espinoza-Fonseca LM. Sarcolipin Promotes Uncoupling of the SERCA Ca(2+) Pump by Inducing a Structural Rearrangement in the Energy-Transduction Domain. Biochemistry 2016;55(44):6083–6.
[19] Wang S, Gopinath T, Larsen EK, Weber DK, Walker C, Uddigiri VR, et al. Structural basis for sarcolipin's regulation of muscle thermogenesis by the sarcoplasmic reticulum Ca 2+ -ATPase. Sci. Adv. 2021;7(48). https://doi.org/10.1126/sciadv.abi7154.
[20] Aguayo-Ortiz R, Fernández-de Gortari E, Espinoza-Fonseca LM. Conserved Luminal C-Terminal Domain Dynamically Controls Interdomain Communication in Sarcolipin. J Chem Inf Model 2020;60(8):3985–91.
[21] Gloster J, Harris P. The lipid composition of mitochondrial and microsomal fractions from human ventricular myocardium. J Mol Cell Cardiol 1970;1:459–65.
[22] Gloster J, Harris P. The lipid composition of subcellular fractions from different chambers of the dog's heart. J Mol Cell Cardiol 1971;2:21–30.
[23] Mani R, Cady SD, Tang M, Waring AJ, Lehrer RI, Hong M. Membrane-dependent oligomeric structure and pore formation of a beta-hairpin antimicrobial peptide in lipid bilayers from solid-state NMR. Proc Natl Acad Sci U S A 2006;103(44):16242–7.
[24] Koch D, Alexandrovich A, Funk F, Kho AL, Schmitt JP, Gautel M. Molecular noise filtering in the beta-adrenergic signaling network by phospholamban pentamers. Cell Rep 2021;36:109448.
[25] Forrest LR. Structural Symmetry in Membrane Proteins. Annu Rev Biophys 2015;44(1):311–37.
[26] Lian P, Wei D-Q, Wang J-F, Chou K-C, Flower DR. An allosteric mechanism inferred from molecular dynamics simulations on phospholamban pentamer in lipid membranes. PLoS ONE 2011;6(4):e18587. https://doi.org/10.1371/journal.pone.001858710.1371/journal.pone.0018587.g00110.1371/journal.pone.0018587.g00210.1371/journal.pone.0018587.g00310.1371/journal.pone.0018587.g004.
[27] Cleary SR, Fang X, Cho EE, Pribadi MP, Seflova J, Beach JR, Kekenes-Huskey P, and Robia SL, Inhibitory and Stimulatory Micropeptides Preferentially Bind to Different Conformations of the Cardiac Calcium Pump. BioRxiv 2021;2021.06.15.448555.